

Electronic Supplementary Information (ESI)

Ultrafine Platinum/Iron Oxide Nanoconjugates Confined in Silica Nanoshells for Highly-Durable Catalytic Oxidation

Hongyu Zhao,^a Dawei Wang,^b Chuanbo Gao,^{*a} Hongyang Liu,^{*c} Lu Han,^d and Yadong Yin^{*b}

^aCenter for Materials Chemistry, Frontier Institute of Science and Technology, Xi'an Jiaotong University, Xi'an, Shaanxi 710054, China. E-mail: gaochuanbo@mail.xjtu.edu.cn

^bDepartment of Chemistry, University of California, Riverside, California 92521, United States. Email: yadong.yin@ucr.edu

^cShenyang National Laboratory for Materials Science, Institute of Metal Research, Chinese Academy of Sciences, Shenyang, Liaoning 110016, China. E-mail: liuhy@imr.ac.cn

^dSchool of Chemistry and Chemical Engineering, Shanghai Jiao Tong University, Shanghai 200240, China

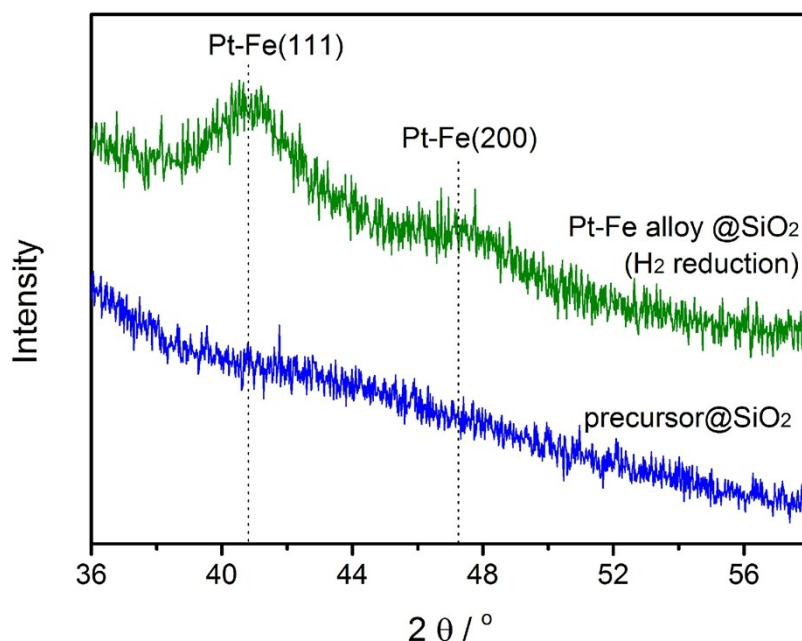


Figure S1. XRD patterns of the precursor@SiO₂ multi-core/shell nanospheres and the Pt-Fe alloy@SiO₂ yolk/shell nanospheres. The Pt-Fe alloy@SiO₂ yolk/shell nanospheres were obtained by annealing the precursor@SiO₂ nanospheres in H₂ (5% in N₂) at 600 °C for 3 h. The shift of the X-ray reflection peaks from pure Pt ones confirmed the formation of Pt-Fe alloy nanoparticles.

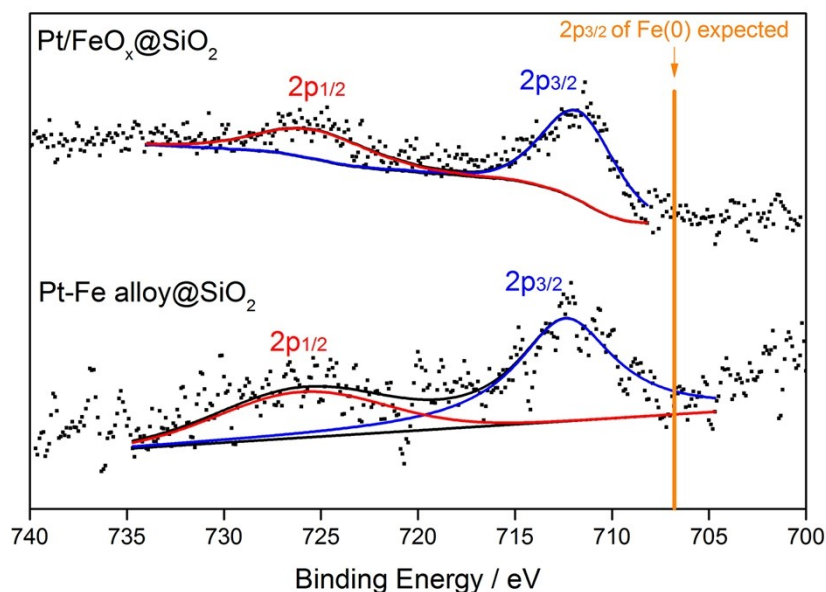


Figure S2. Fe 2p XPS spectra of the Pt-Fe alloy@SiO₂ and Pt/FeO_x@SiO₂ nanospheres. Peaks of Fe(III) (2p_{3/2} ~712 eV, 2p_{1/2} ~726 eV) can be clearly observed from both samples, indicating that Fe(III) species exists during the whole alloying and dealloying process during the synthesis of the Pt/FeO_x@SiO₂ yolk/shell nanospheres. It can be attributed to the presence of a portion of Fe species that were diffused into the silica shell in the form of a silicate during the reduction and re-oxidation processes. It is worth noting that XPS did not show clear signals from Fe(0) in the Pt-Fe alloy@SiO₂ nanospheres, which can be attributed to the large portion of the diffused Fe(III) species at the surface, while Fe(0) species were in the core and in a relatively low abundance. However, this relatively low abundance of Fe(0) in the Pt-Fe alloys proved to be effective to yield Pt/FeO_x nanoconjugates with close interfaces after the dealloying process.

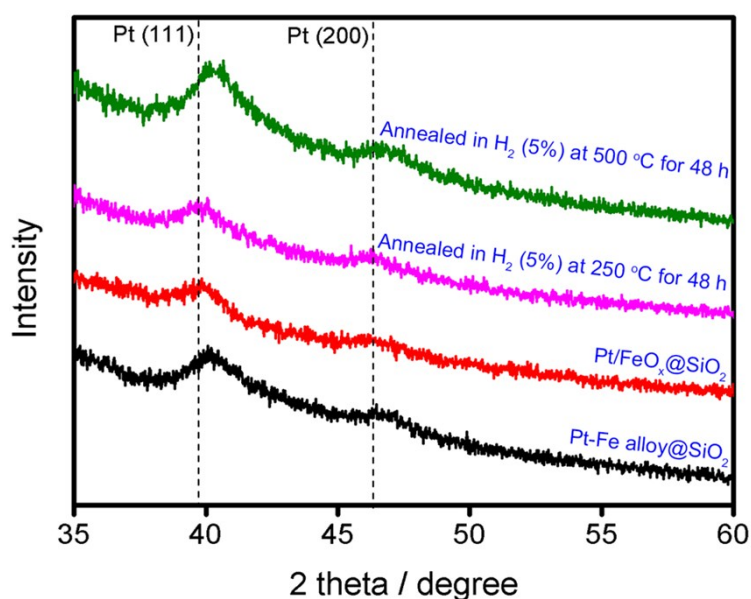


Figure S3. XRD patterns of the Pt/FeO_x@SiO₂ core/shell nanospheres after annealing in reductive atmosphere (H₂, 5%; N₂, 95%) at different temperatures for 48 h. The sample

annealed at 250 °C showed almost no change in the XRD pattern, suggesting that the Pt/FeO_x nanostructure remained stable. After annealing at 500 °C for 48 h, the iron oxide was reduced and alloyed with Pt, showing a typical XRD pattern of Pt-Fe alloy nanoparticles. The catalyst was therefore stable in reductive atmosphere at relatively low reaction temperatures.

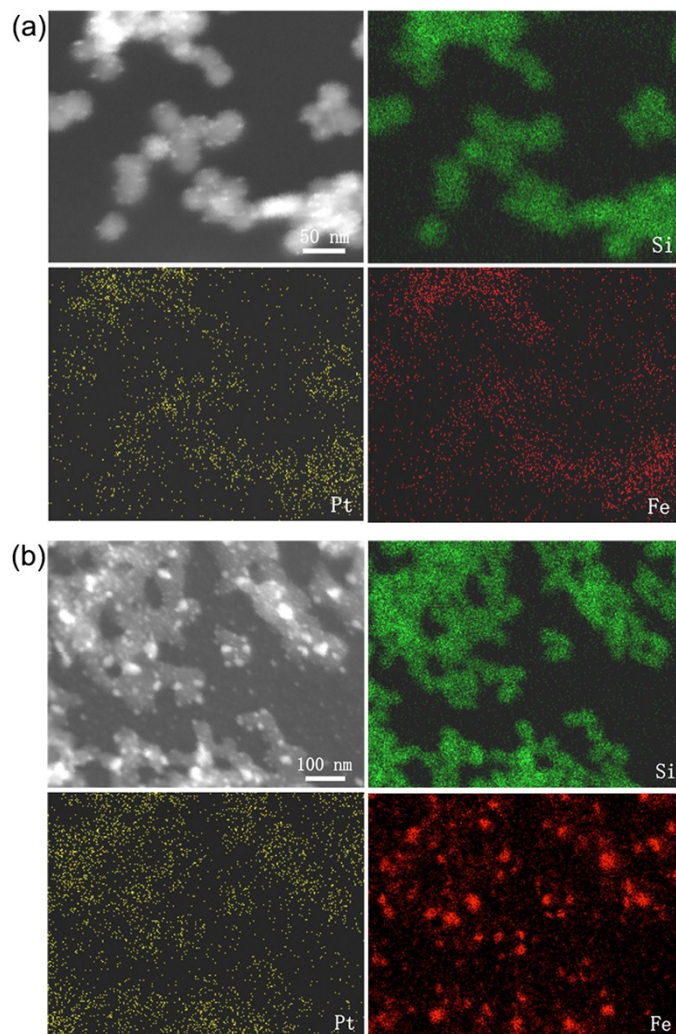


Figure S4. Thermal instability of the surface-stabilized Pt/FeO_x nanoconjugates (SiO₂/Pt/FeO_x) investigated by EDS elemental mapping. (a) HADDF, distributions of Si, Pt and Fe of the original SiO₂/Pt/FeO_x catalyst before thermal treatment, showing that the Pt and FeO_x nanoparticles were uniformly distributed on the silica carrier without aggregation. (b) HAADF, distributions of Si, Pt and Fe of the SiO₂/Pt/FeO_x catalyst after thermal treatment at 500 °C, which showed obvious agglomeration of the FeO_x nanoparticles. It is therefore concluded that the surface-stabilized Pt/FeO_x nanoconjugates are prone to sintering at elevated reaction temperatures.

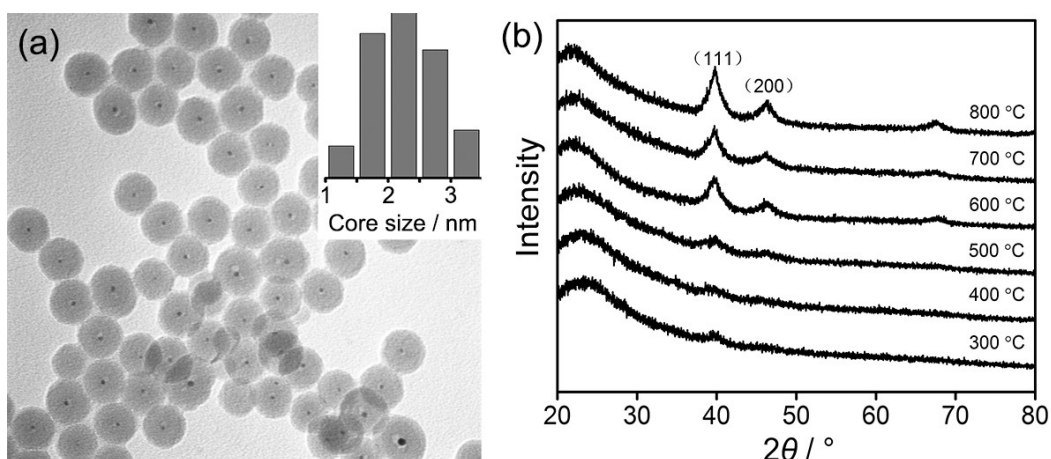


Figure S5. Monometallic Pt@SiO₂ core/shell nanospheres. The sample was obtained without adding FeCl₃ in a typical synthesis, and was employed as a control catalyst in PROX. (a) A TEM image of the Pt@SiO₂ core/shell nanospheres obtained after annealing at 600 °C in air for 1 h. Inset: core size distributions. (b) XRD patterns of the samples annealed in air for 1 h at different temperatures. The results indicate that (NH₄)₂PtCl₆ nanoparticles were well decomposed into Pt nanoparticles at a temperature above 600 °C.

Table S1. Elemental analysis of the Pt/FeO_x@SiO₂ yolk/shell nanospheres and the Pt@SiO₂ core/shell nanospheres.

Entry	Pt / mmol g ⁻¹	Fe / mmol g ⁻¹
Pt/FeO _x @SiO ₂	0.160 ^a	0.440 ^a
Pt@SiO ₂	0.156 ^a	—
SiO ₂ /Pt/FeO _x	0.205 ^b	0.090 ^b

^aMeasured by ICP-MS.
^bMeasured by EDS.

Additional notes to Table S1:

(1) The Pt/Fe ratio of the catalyst SiO₂/Pt/FeO_x is larger than the catalyst Pt/FeO_x@SiO₂. The ratio was chosen because the catalyst SiO₂/Pt/FeO_x showed optimal catalytic activities in PROX among catalysts of different ratios (Reference: *Science* 2010, 328, 1141), which makes the catalyst an appropriate benchmark for evaluating the catalytic activities of the encapsulated catalysts developed in this work.

(2) The same amount of the catalysts was used in each run of the catalysis. When evaluating the catalytic activity of the catalyst Pt/FeO_x@SiO₂ in comparison with the control catalyst, SiO₂/Pt/FeO_x, the Pt-specific catalytic activities of the encapsulated catalyst Pt/FeO_x@SiO₂ can be even higher than that indicated by Figure 6a.